ACS APPLIED MATERIALS & INTERFACES

RESEARCH ARTICLE

www.acsami.org

Preparation and Characterization of Monodispersed Microfloccules of TiO_2 Nanoparticles with Immobilized Multienzymes

Min Wu,*[,†] Qin He,[†] Qianfei Shao,[‡] Yonggang Zuo,[†] Fen Wang,[†] and Henmei Ni[†]

[†]School of Chemistry and Chemical Engineering, Southeast University, Nanjing 211189, China

[‡]Anhui Lixing Chemical Co., Ltd., Anhui, 245300, China

ABSTRACT: Microfloccules of TiO_2 nanoparticles, on which glycerol-dehydrogenase (GDH), 1,3-propanediol-oxidoreductase (PDOR), and glycerol-dehydratase (GDHt) were coimmobilized, were prepared by adsorption-flocculation with polyacrylamide (PAM). The catalytic activity of immobilized enzyme in the glycerol redox reaction system, the enzyme leakage, stabilities of pH and temperature, as well as catalytic kinetics of immobilized enzymes relative to the free enzymes were evaluated. Enzyme loading on the microfloccules as much as 104.1 mg/g TiO_2 (>90% loading efficiency) was obtained under the optimal conditions. PAM played a key role for the formation of microfloccules with relatively homogeneous distribution of size and reducing the enzyme leakage from the microfloccules during the catalysis reaction. The stabilities of GDH against pH and temperature was significantly higher than that those of free GDH. Kinetic study demonstrated that simultaneous NAD(H) regeneration was feasible in glycerol redox system catalysted by these multienzyme microfloccules and the yield of 1, 3-popanediol (1, 3-PD) was up to 11.62 g/L. These results indicated that the porous and easy-separation microfloccules of TiO_2 nanoparticles with immobilized multienzymes were efficient in term of catalytic activity as much as the free enzymes. Moreover, compared with free enzyme, the immobilized multienzymes system exhibited the broader pH, higher temperature stability.

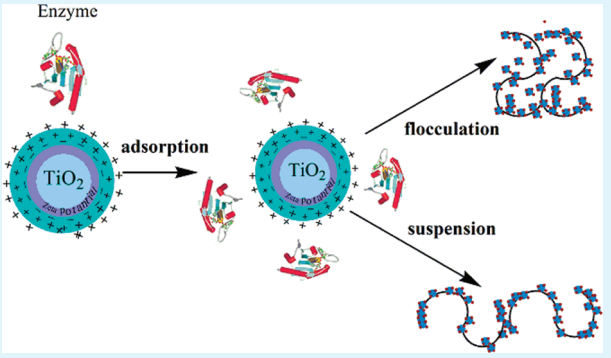

KEYWORDS: multienzyme, microfloccule, kinetics, nano/microstructure, cofactor regeneration, 1,3-popanediol

1. INTRODUCTION

1,3-PD is typically biobased bulk chemicals that have been used as monomer to produce polyester polyol PTT, a promising biodegradation material in recent years.[1,2] Biosynthesis of 1,3-PD has many advantages such as the use of renewable resources as raw material, the low carbon emission and the selective specificity. Cells fermentation has been industrially applied to produce 1,3-PD as a competitor to the traditional petrochemical routes. In the cell fermentation process, it has been proved that three enzymes eventually play the key role for the conversion of glycerol to 1,3-PD in a pathway of glycerol dismutation by *Klebsiella pneumoniae*, i.e., glycerol-dehydrogenase (GDH, EC 1.1.1.6), 1,3-propanediol-oxidoreductase (PDOR, EC 1.1.1.202), and glycerol-dehydratase (GDHt, EC 4.2.1.30), whereas the coenzyme $NAD^+/NADH_2$ simultaneously regenerated coupling with glycerol redox system.[3,4]

Theoretical sketch of this bioprocess is shown in Figure 1,[5,6] glycerol is dissimilated through oxidative and reductive pathways, coupled with regeneration of coenzyme NAD(H). Naturally, coenzymes NAD(H) and NADP(H) generally act as electron carriers facilitating such redox biotransformation, and the native cofactors are often much more expensive.[7]

Therefore, it is natural to consider an alternative method directly using the multienzymes system instead of cell fermentation as the future development of biosynthesis, because compared

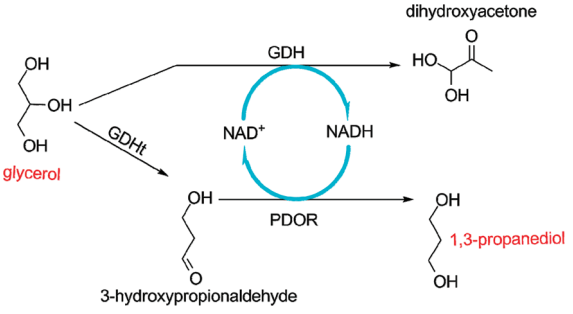

Figure 1. Cofactor regeneration within metabolic pathway of biocatalysising glycerol to 1, 3-PD.

with the cell fermentation, the enzyme synthesis[8] is advantageous to the lower cost, simple operation, no cell pollution as well as the benefit of continuity of operation and successive separation. Some efforts have been made to immobilize multienzyme systems via nanoporous carriers coupling with cofactors regeneration.[9,10] Nanoparticles are usually considered as the ideal carriers, on which the enzymes are immobilized. The large ratio of surface

Received: December 15, 2010
Accepted: August 4, 2011
Published: August 04, 2011

area-volume of nanoparticle renders the immobilization of enzymes to perform under the moderate conditions which are essential to impose the least effect on the natural morphologies of enzyme, in turn to keep the activity.[11−14] In addition, nanoscale size of carrier can be readily dispersed in the reaction system, thus may provide the sufficient time and space for the contact of enzyme and other reagents. Last but not least, nanoparticles are of good biocompatibility, low cost, and easy availability, and provide an ideal remedy to the usually contradictory issues encountered in the optimization of immobilized enzymes.[15−18] For example, nano-TiO_2 has been investigated and proved to be an ideal enzyme carrier because of its high chemical and thermal stability and good compatibility with the environment.[19,20]

However, the recovery of nanoparticles after the reaction are often daunting tasks. Additionally, the high leakage of enzyme due to its open structure significantly restricts their application in enzyme immobilization. Nowadays, organic−inorganic hybrid materials have emerged as a novel class of materials, which may find promising applications for enzyme immobilization with the potential use in biomedical, biocatalysis, bioseparation, and biosensing areas.[21−24] In fact, it did be demonstrated that the enzyme immobilized by organic−inorganic hybrid carrier maintained viability in measuring process.[25−27] These results implied a concept that the enzyme carrier with microsize may be better than the nanocarrier due to the easy separation, coupling with the similar efficiency to the nanocarrier. Therefore, in this paper, we will have a trial to prepare the microfloccules of nano-TiO_2 immobilizing enzymes and use them as catalyst in the biosynthesis of 1,3-PD. The loose and porous structure of hybrid microfloccules is expected to integrate the three enzymes, i.e., GDH, PDOR, and GDHt, and cofactor into molecular vicinity,[28−30] and thus enable effective translocation of the cofactor between the active sites of the two coimmobilized enzymes.

2. MATERIALS AND METHODS

2.1. Materials. Nano-TiO_2 (14 nm) with surface area of 280 m^2/g (BET method) was prepared in our lab. Bovine serum albumin (BSA), NAD^+, and VB_{12} were purchased from Sigma Chemical Co. Ltd. A 0.05% (w/v) aqueous solution of MBTH (3-methyl-2-benzothiazolinone hydrazone) was freshly prepared by dissolving the requisite amount of MBTH (Merck, Germany) in distilled water and stored in dark colored bottle. Glycerol, 1,3-propanediol, Tris(hydroxymethyl)aminoethane (99.5%) and Polyacrylamide (cPAM, Mn = 12 × 10^6, aPAM, Mn = 12 × 10^6, nPAM, Mn = 9 × 10^6, commercial grade) were obtained from Sinopharm Chemical Reagent Co., Ltd. All reagents were used without further purification.

2.2. Extraction of Enzymes. The enzymes were extracted as following: collecting K. pneumonia cells by centrifugation (4 °C, 20 min at 4000 × g) followed with washing twice with 50 mM Tris-HCl buffer solution (pH 7.0), and then suspending cells in buffer solution up to an concentration of 5 g/L. After proliferation, the crude enzyme was extracted by ultrasonic-centrifugation separation of cells at 8000 × g and then desalted with 30−70% saturated $(NH_4)_2SO_4$. The activity of enzyme salted out by each concentration of saturated $(NH_4)_2SO_4$ was measured.[31] All the maximum activities of GDH, GDHt and PDOR were in the vicinity of 50%. Therefore, 50% saturated $(NH_4)_2SO_4$ was employed for the crude enzyme extract in this work. The multienzyme was dissolved and stored in 50 mM pH 7.0 Tris-HCl buffer solution at 4 °C.

2.3. Preparation of Microfloccules with Immobilized Multienzymes. After mixing 0.2 g of TiO_2 and 1.0 mL of multienzyme solution (20 mg/mL) at 37 °C and 180 rpm for 30 min, 2.0 mL 0.25 mg/mL PAM solution was added and shook continuously for 30 min. The floccule was centrifugated at 4000 × g and washed with 50 mM Tris-HCl buffer solution until no protein was detectable in the solution. The floccule with immobilized multienzymes was stored at 4 °C before it was used.

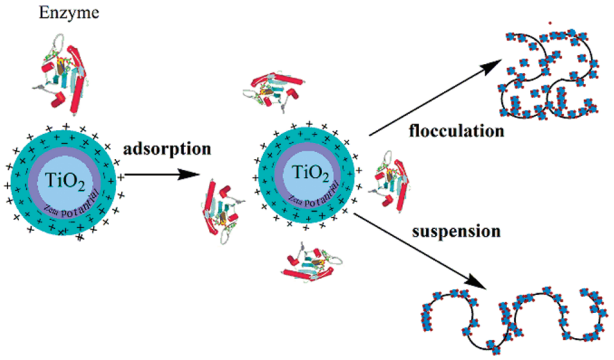

Figure 2. Schematic diagram of PAM-TiO_2 microfloccules with immobilized enzymes.

2.4. Quantitative Analysis of Microfloccules. *2.4.1. Assays of Enzyme Activity of the Microfloccules and Free Enzymes.* The activity of GDH and PDOR was determined spectrophotometrically (340 nm) at 37 °C by the initial rate of substrate-dependent NADH formation according to the references.[31,32] The assay mixtures for GDH contained in a 5-mL final volume: 200 mM glycerol (substrate), 2 mM NAD^+, 30 mM $(NH_4)_2SO_4$, 1 μM $(NH_4)_2Fe(SO_4)_2$, and 100 mM K_2CO_3 buffer at pH 12.0. Units of activity are given in micromoles per min at 37 °C.

The method for the activity of PDOR was the same as that of GDH, except that the standard assay was carried out in 100 mM 1,3-propanediol (substrate) and 100 mM K_2CO_3 buffer at pH 9.5.

The GDHt assay mixture contained 50 mM KCl, 200 mM 1,2-propanediol, 15 μM VB_{12}, and 35 mM potassium phosphate buffer solution (pH 7.0). The assay was started by adding enzyme extract with a dehydration time about 10 min, and then terminated by adding potassium citrate buffer (pH 3.6). After 15 min incubation with MBTH solution, the colored azin was determined spectrophotometrically at 305 nm following the procedure of Ahrens et al.[31,4]

2.4.2. Loading Efficiency and Loading Amount. Enzyme loading and loading efficiency on the carrier were determined by detecting the protein content in the solution (including the washing solution) before and after immobilization. Bradford method was employed by using bovine serum albumin (BSA) as the standard. The loading efficiency, loading amount, residual activity and relative activity of immobilized enzyme were calculated with eqs 1−4, where W is the quality and U refers to enzyme activity.

$$\mathrm{enzymeloadingefficiency} = \frac{W_{\mathrm{initialenzyme}} - W_{\mathrm{endenzyme}}}{W_{\mathrm{initialenzyme}}} \times 100\% \quad (1)$$

$$\mathrm{enzymeloadingamount} = \frac{W_{\mathrm{initialenzyme}} - W_{\mathrm{endenzyme}}}{W_{\mathrm{TiO2}}}\ (\mathrm{mg/g}) \quad (2)$$

$$\mathrm{residualactivity} = \frac{U_{\mathrm{immobilizedenzyme}}}{U_{\mathrm{initialenzymeusedforimmobilization}}} \times 100\% \quad (3)$$

$$\mathrm{relativeenzymeactivity} = \frac{U_{\mathrm{anygroupinparallelexperiments}}}{U_{\mathrm{higestenzymeactivity}}} \times 100\% \quad (4)$$

2.4.3. pH and Tempreture Stability. Stabilities of free and immobilized enzyme against pH were evaluated in light of the catalytic activity of enzyme by adding 13.6 mg of immobilized enzyme to 2.2 mL of 100 mM

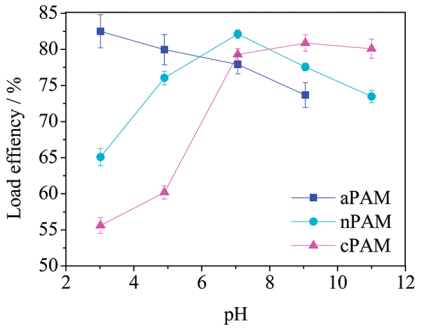

Figure 3. Effect of pH on the flocculation behavior of polyacrylamide.

buffer, after being incubated at 37 °C for 1 h in buffers with pH from 5.0 to 10.0,[33−35] the residual activities were determined.

Similar to evaluation of pH stability, enzymes were incubated in pH 7.0 buffers at 4 to 70 °C for 1 h and then their residually activities were determined.

2.4.4. Catalytic Kinetics of Immobilized Enzymes. GDH-catalyzed oxidation of glycerol to dihydroxyacetone coupling with the reduction of NAD^+ to NADH (eq 5) and PDOR-catalyzed oxidation of 1, 3-PD to 3-hydroxypropionaldehyde coupling with the reduction of NAD^+ to NADH for immobilized GDH and PDOR (eq 6) were shown below.[31,33]

$$C_3H_8O_3 + NAD^+ \rightleftharpoons C_3H_6O_3 + NADH + H^+ \quad (5)$$

$$C_3H_8O_2 + NAD^+ \rightleftharpoons C_3H_6O_2 + NADH + H^+ \quad (6)$$

The maximum rate of reaction (V_{max}) and Michaelis−Menten constant (K_m) for free and immobilized GDH (eq 5) were determined by using Lineweaver−Burk plot. The enzyme activity was determined spectrophotometrically by directly measuring the decrease of absorbance of NADH at 340 nm. The conditions were same as those described in section of "2.4.1"

Full time records were also analyzed, from which kinetic constants at given substrate concentrations could be obtained. For the kinetics study, a range of 1,3-PD concentrations (eq 6) from 10 to 50 mM was assayed. A unit of PDOR activity was defined as the amount of enzyme required for the formation of 1 μmol of NADH per min at 37 °C.

2.5. Characterization of Microfloccules. Scanning electron microscopy (SEM, S-4800, Hitach High-Tech Ltd., Tokyo) was employed to observe the morphology and the spatial distribution of sulfur element of microfloccules. Different from the common sample preparation,[37] the hybrid powder of microfloccules that dried at 60 °C by vacuum was observed directly without any sputter gold-coating. Elemental analysis was determined by energy-dispersive spectroscopy (EDS) analysis attached to the SEM.

The size and its distribution of microfloccules was determined by concentrated dispersed systems (Electroacoustic spectrometer DT 1200, Dispersion Technology Inc., USA). Microfloccule dispersions (5 wt %) suspended in water (pH 7.0) with total volume of 100 mL was poured into the DT-1200 measuring chamber equipped with a magnetic stirrer for preventing sample sedimentation and the multiple statistical measurements of particle size distribution (PSD) were treated automatically by the machine. The data of at least three measurements were used.

2.6. Production of 1,3-Propanediol by Microfloccules with Immobilized Multienzymes. One and a half grams of microfloccules was put into 50 mL of initial reaction solution and the mixture was then incubated at 37 °C and 180 rpm for 10 h. Periodically, 1 mL of the reaction solution was sampled and centrifuged at 8000 × g for 10 min. 1,3-propanediol concentration was determined by GC. A typical initial reaction solution contained: glycerol 25 g/L, NAD^+ 2 mM, VB_{12} 15 μM,

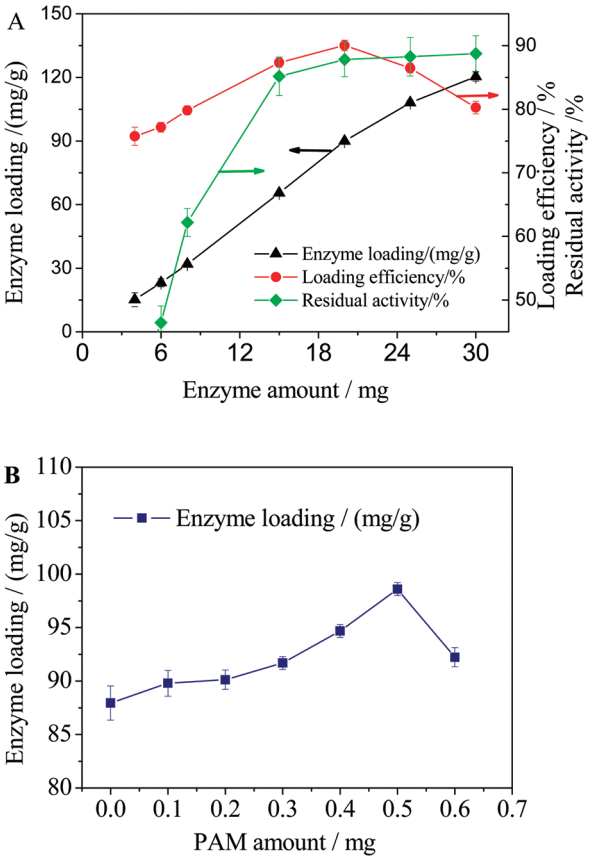

Figure 4. Effect of enzyme and nPAM amount on the immobilization. (A) Effect of enzyme amount on the loading, loading efficiency, and residual activities. (B) Effect of nPAM amount on the loading.

$(NH_4)_2SO_4$ 30 mM, $(NH_4)_2Fe(SO_4)_2$ 1 μM, Mg^{2+} 1.7 mM, and pH 8.0 Tris-HCl buffering solution.

3. RESULTS AND DISCUSSION

3.1. Preparation of Microfloccules. *3.1.1. Effect of Enzyme Amount and PAM on the Immobilization.* PAM was a well-known flocculating agent for purification of water and flocculation cells.[36] $CONH_2$ groups in PAM chains intensively interacted with the COOH groups by H-bonds even in the aqueous solution, in addition to the entanglement of PAM chains, i.e., the bridge effect, which in turn to result in the formation of insoluble complexes.[37,38] For this reason, we selected PAM as the flocculating agents to prepare the microfloccules of nano-TiO_2 particles, expecting the interaction of PAM and enzymes containing COOH groups to further prevent the adsorbed enzymes from leaking. The process and structure of microfloccules with immobilize enzymes are schematically shown in Figure 2. Such loose structure was expected to provide the free space as much as possible for the access of substrate molecules, besides the merit of recovering enzymes.

However, it should be remarked that the flocculation depended on both the concentration and types of PAM. At the low concentration, the entanglement of PAM chains cannot occur, thus the microfloccules cannot form. Therefore, in this paper, for the comparisons, the data of loading efficiency of enzymes at the low concentration of PAM was obtained from the species of nanoparticles ultracentrifuged at 8000 × g. Certainly, in order to decrease the disentangle concentration of PAM, the length of

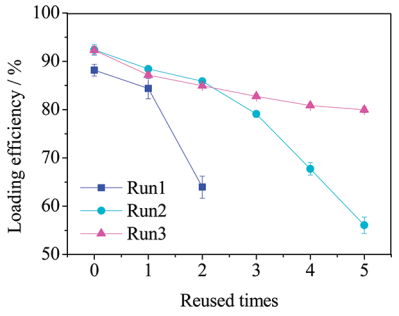

Figure 5. Stability experiment for microfloccules of nano-TiO_2 immobilizing enzymes.

PAM chains was intentionally selected as long as possible. This was the reason that PAM with nearly MW of 1×10^7 was used in this paper.

On the other hand, the flocculation of nanoparticles was caused by interactions between the polymer chains and nanoparticles, namely the bridge effect of polymer chain. Therefore, to investigate the interactions, three types of PAM, i.e., cationic, anionic, and nonionic PAM were chosen preliminarily for the flocculation of TiO_2 nanoparticles. The different end groups may also affect the flocculation performance of PAM. The results were showed in Figure 3. As shown in Figure 3, the highest efficiencies of enzyme loading were all around 80−84%, regardless of the types of PAM. However, the performance of flocculation against pH was quite different. For anionic PAM (aPAM), the flocculation did not occur at high pH, whereas for cationic PAM (cPAM), the big aggregation, instead of microfloccules, formed. It is normal that the flocculation of nanoparticles was dependent to the bridge-effect of polymer, and further, the anchor-effect of electrostatic or polar interactions of polymer chains and TiO_2 nanoparticles played the key role in the bridge-effect.[39−41] The charges on the surface of TiO_2 nanoparticles were positive at low pH and negative at high pHs. Therefore, by using aPAM and cPAM, the electrostatic interactions dominated the flocculation behavior, whereas for nonionic PAM (nPAM), the polar interactions were dominant. In the case of polar interaction, the net charges on TiO_2 nanoparticles played the roles both for the stabilization and the loose or porous structure of microfloccules. This was the reason that by using nPAM, the compact microfloccules could form in a wide range of pHs, and we concluded to choose the nPAM as the floccutant for the preparation of microfloccules in this work.

The effect of enzyme and PAM amount on the enzyme loading was shown in Figure 4. As shown in Figure 4A, the enzymes loading increased with the increase of enzymes amount added into the solution, but the loading efficiency decreased when the added amount of enzymes was over 20 mg. The maximum loading efficiency was 90.02% corresponding to the loading amount of 90.02 mg/g of TiO_2. Although the loading amount slightly increased with the increase of charged amount of enzymes, it did not mean the maximum loading amount was the best in application. As shown in Figure 4A, the residual activity of immobilized enzymes increased to the highest value at 20 mg, and then leveled off with the increase of charged amount of enzymes. The strong relationship of residual activity with the concentration of active enzymes was attributed to the density of enzymes adsorbed on the surface of nano-TiO_2 particles. The overdense adsorption may envelop the active center of enzymes

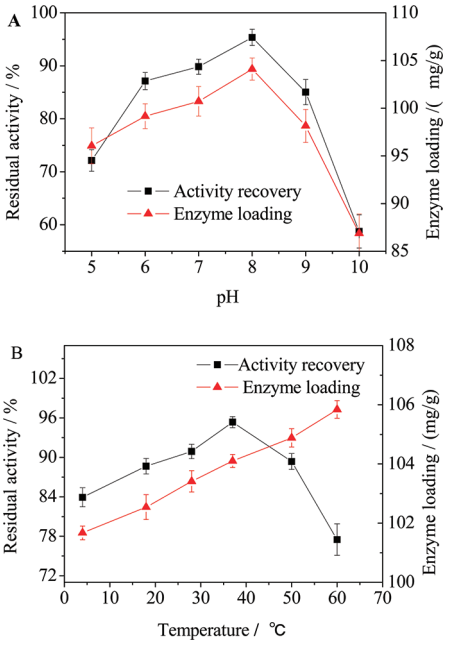

Figure 6. Effect of pH and temperature on residual activities and enzyme loading.

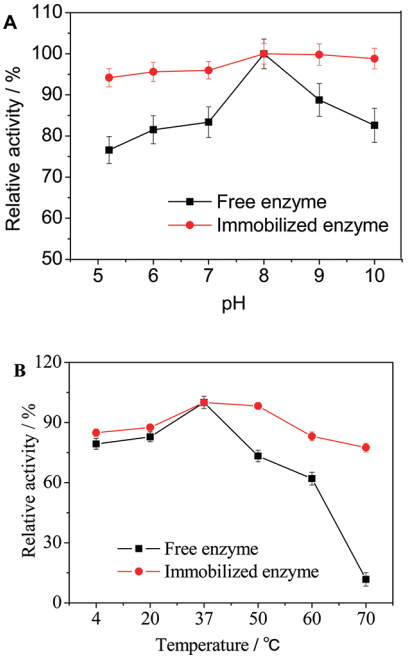

Figure 7. pH and thermal stabilities of free and immobilized GDH at the given temperature and pH on the relative activity.

and consequentially decrease the activity of enzymes. Therefore, we considered that 90.02 mg/g of TiO_2 was the amount of saturated adsorption and the optimal amount of loading.

On the basis of the optimal amount of loading, the effect of adding nPAM was investigated. As shown in Figure 4B, the loading amount slightly increased with the increase of PAM amount until 0.5 mg PAM was added, and then abruptly decreased. It was obvious that PAM could impact the loading

amount of enzymes by the formation of microfloccules. We should point out that, when the amount of PAM was lower than 0.2 mg, ultracentrifugation was needed to separate the nanoparticles with immobilized enzymes. However, when the amount of PAM was between 0.2−0.5 mg, the microfloccules were formed and easily separated by filtration. It indicated that 0.2 mg of PAM was the critical concentration for flocculation in this system. On the other hand, as shown in Figure 4B, adding PAM more than 0.5 mg, the loading amount dramatically decreased. It was understandable readily that the free PAM in the aqueous phase consumed some enzymes.

Anyway, for brief, the change of loading efficiency was not shown in Figure 4B because the trend line of loading efficiency was consentaneous with loading amount plot. As a result, the highest loading amount as much as 98.59 mg/g of TiO_2 particles (corresponding to the maximum loading efficiency of 98.05%) with PAM amount of 0.5 mg was obtained.

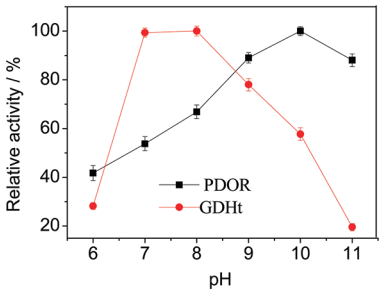

Figure 8. pH stability of immobilized PDOR and GDHt.

However, after all, the leakage of enzymes from microfloccules in practice should be considered. To investigate the cause of leakage, we did three experiments, respectively. In Run 1, the aggregating blocks of TiO_2 nanoparticles with enzymes were prepared by ultracentrifugation without PAM, and then applied for the catalytic reaction. In Run 2, the above microfloccules were repeatedly used. In Run 3, PAM was added at the moment when recovering the microfloccules. The results are showed in Figure 5. The consistent term of loading efficiency was applied for evaluating the leakage of enzymes, namely measuring the concentration of enzymes in the reaction solution and then calculating the loading efficiency of residual enzymes in the microfloccules. As shown in Figure 5, Run 1 indicated that the enzyme loading efficiency decreased dramatically after repeated use, whereas Run 3 showed the slight decrease of loading efficiency against the repeated times. In fact, the aggregating blocks of TiO_2 nanoparticles with immobilized enzymes prepared by ultracentrifugation without PAM decomposed when they were dispersed in the reaction system. Obviously, the leakage of enzymes was remarkably abated by adding PAM. These results indicated that the leakage of enzymes during the repeated applications was likely resulted from the escaping nanoparticles of TiO_2-enzymes from the microfloccules bound by PAM. The lost of PAM might also contribute to the leakage of enzymes because of the formation of

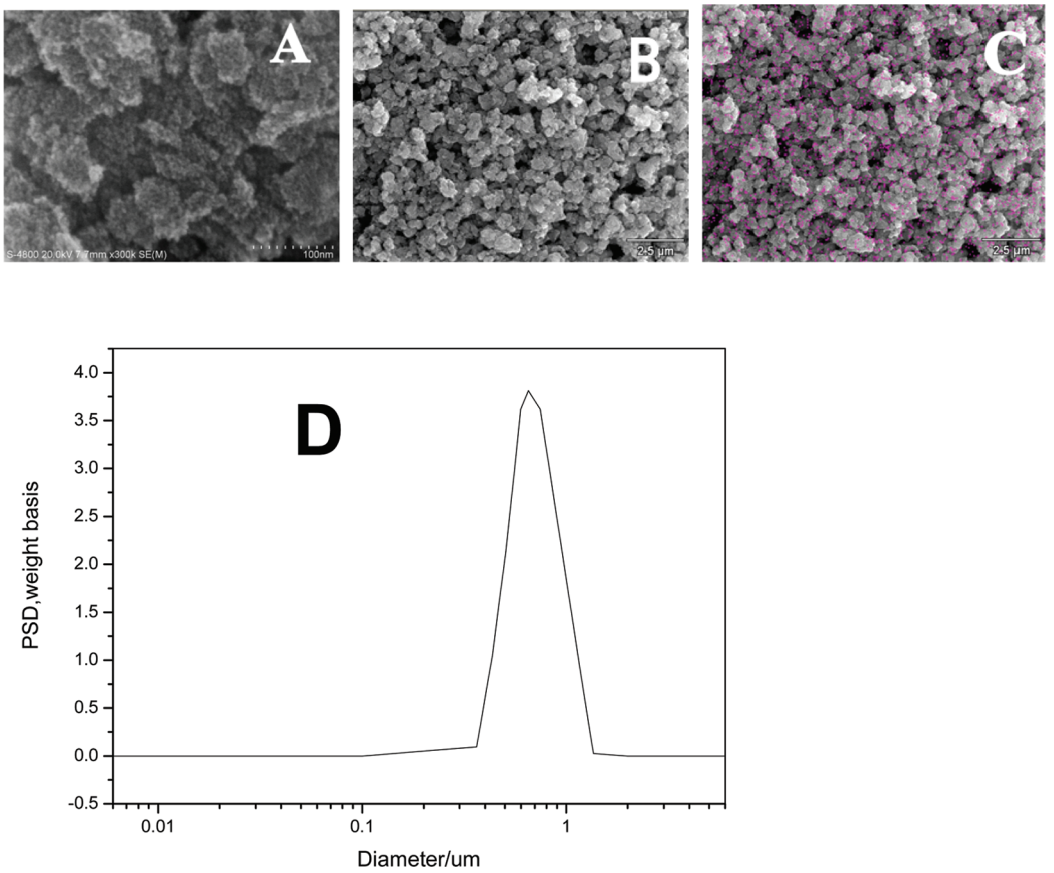

Figure 9. SEM images of nano-TiO_2 (A), immobilized multienzyme particles (B), sulfur element dot mapping of enzyme immobilized hybrid PAM-TiO_2 gel taken by EDS (C) Inset: EDS spectra of immobilized multienzyme, and (D) particle size distribution measured by electroacoustic spectrometer in aqueous media.

PAM-enzymes complexes. However, at pH 8, the interaction of H-bond between enzyme-COOH and PAM was very weak.[37] Hence, it might be negligible.

3.1.2. Effect of pH and Temperature on the Immobilization. In the above section, the highest loading amount of enzymes was obtained, e.g., 98.59 mg/g of TiO_2 particles under the conditions of 0.5 mg PAM at 37 °C and pH 7.0. In this section, we will investigate the effects of pH and temperature on the loading amount as well as the activity of enzymes with the constant PAM amount (0.5 mg of PAM/200 mg of TiO_2 particles).

The effects of pH on the loading amount and apparent activity of immobilized GDH at 37 °C are shown in Figure 6A. Obviously, pH affected both the loading amount and the activity of GDH. Maximum activity was 95.36% at pH 8.0 corresponding to the maximum enzyme loading of 104.1 mg/g. It was attributed to the change of charges on the nanoparticles as well as in the polymer chains of GDH and PAM caused by pH. Low pH unfavored the dissociation of COOH, thus enhanced the interaction of PAM with COOH,[37,38,42−44] but meanwhile, it also destroyed the double layer of nano-TiO_2 particles as well as the morphology of GDH. The balance of these two inverse actions determined the maximum activity of enzyme as well as the loading amount. At the higher pH (>8.0), the low activity of enzyme might be attributed to the low amount of enzymes, whereas in contrast, at the lower pH, mechanisms of the attenuated GDH activity might be ascribed to the changed protein folding and binding modes (electrostatic or via hydrogen bonds) .

Figure 6B shows the effects of temperature on the loading amount and apparent activity of immobilized GDH at pH 8.0. It was clear that enzyme loading amount increased slightly with the temperature rising from 4 to 60 °C, whereas apparent activity was reached maximum at 37 °C. This result indicated that the temperature less affected the loading amount.

By these two results, it was concluded that optimum conditions of immobilization were pH 8.0 at 37 °C, under which the loading amount and apparent activity of immobilized GDH were 104.1 mg/g and 95.36%, respectively.

Table 1. Each Element Content in Immobilized Enzyme

element	weight (%)	atomic (%)
C K	43.92	58.20
N K	19.74	22.43
Al K	28.03	16.54
S K	0.47	0.23
Ti K	7.84	2.61
Total	100.00	100.00

3.2. Stability Against pH and Temperature of the Microfloccules and Free Enzymes. In this section, we will compare the stability of free GDH with the immobilized GDH. The residual activity of GDH was measured after free GDH and microfloccules were incubated in the buffer solution with various pHs at 37 °C for 60 min. As the maximum value was taken as 100%, the percentages of residual activity under other conditions, i.e., the relative activity of GDH are shown in Figure 7A. As shown in Figure 7A, the relative activity of immobilized GDH in the microfloccules was almost constant in the pH range from 5.0 to 10.0. For example, at pH 5.0, relative activity of immobilized GDH was 94.16%, whereas 98.84% at pH 10.0. However, inversely the relative activity of free GDH was quite dependent to pH. At pH 8.0, it exhibited the highest value of relative activity, but at other pHs, it showed very low activities. This result indicated that the free GDH was sensitive to pH, whereas the immobilized GDH in the microfloccules not. The reason, we think, may be attributed to the flexible microenvironment within microfloccules.

Stability of temperature on the activity of free and immobilized GDH was also evaluated at pH 8.0 after incubated for 60 min at each temperature. As shown in Figure 7B, the overall temperature−activity profiles of the free and immobilized GDH resembled each other at temperature ranging from 4 to 40 °C. The relative activity slightly increased as the temperature rose. However, when the temperature was higher than 40 °C, the relative activity of both free and immobilized enzyme decreased with the rise of temperature. Even though, comparatively the relative activity of free GDH decreased much more dramatically. For example, at 70 °C, the activity of immobilized GDH retained about 78.0%, whereas that of free one was only 11.7%. If we considered 80% as the proper deadline of activity in practice, this result implied that, relative to the free GDH, the applicable temperature-span of GDH was expanded from 4 to 60 °C by the immobilization in microfloccules.

The relative activity of immobilized PDOR and GDHt were carried out at different pH values ranging from 6.0 to 11.0 (Figure 8). The maximum activity of immobilized PDOR was in range of 9 to11. The highest activity of immobilized GDHt was shown to be in the pH range of 7 to 8 and was markedly reduced

Table 2. Kinetic Parameters for Free and Immobilized GDH

substrate type	state of enzyme	K_m (mM)	V_{max} (mM/min)
NAD^+	free	0.093	0.1004
	immobilized	8.164	0.1043
glycerol	free	0.8794	0.1595
	immobilized	5.4353	0.3103

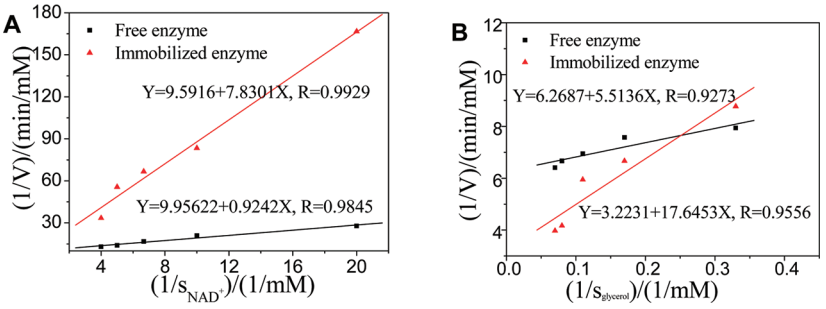

Figure 10. Lineweaver−Burk plots for (A) the NAD^+ reduction and (B) glycerol oxidation with free and immobilized GDH (pH 12.0, at 37 °C).

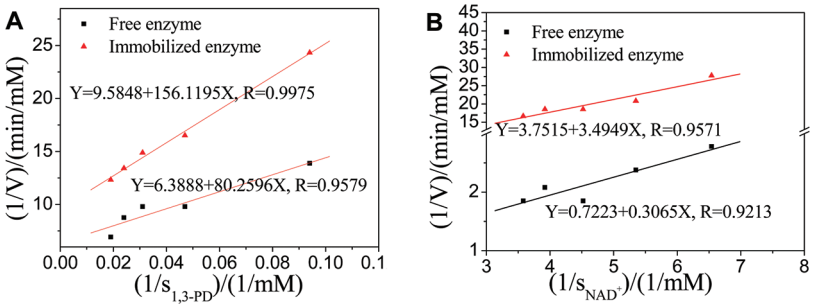

Figure 11. Lineweaver–Burk plots for the (A) 1,3-PD oxidation and (B) NAD^+ reduction with free and immobilized PDOR (pH 9.5, at 37 °C).

Table 3. Kinetic Parameters for Free and Immobilized PDOR

substrate type	state of enzyme	K_m (mM)	V_{max} (mM/min)
NAD^+	free	0.42	1.374
	immobilized	0.82	0.27
1, 3-PD	free	12.60	0.16
	immobilized	16.29	0.11

at relatively lower or higher pH values. In the case of pH stability of coimmobilized GDH, GDHt, PDOR, the proper reaction pH for production of 1,3-propanediol was in range of 8 to 9.

3.3. Morphology of Hybrid Microfloccules. Figure 9 shows the morphology of microfloccules composed of TiO_2/enzyme/PAM hybrid materals. As comparison, the aggregation of pure TiO_2 nanoparticles ultracentrifuged from the aqueous dispersion is also shown in Figure 9A. It is clear that, compared with the big blocks of pure TiO_2 nanoparticles, the hybrid microfloccules were typical porous microparticles.

An assessment of the enzyme distribution in the TiO_2/PAM hybrid was made based on elemental analysis determined by energy dispersive spectroscopy (EDS) analysis attached to the SEM. Figure 9C gives the distribution of sulfur element which represented the adsorbed enzyme proteins on the surface of microfloccules. The concrete data of element distribution are listed in Table 1.

The particle size distribution of as-prepared microfloccules in aqueous dispersion was measured by electroacoustic spectrometer (Figure 9D). These data are in good agreement and show the prevalence of TiO_2/enzyme/PAM hybrid materals with sizes ranging from 500 to 800 nm. These results indicated that, for the preparation of the microfloccules with immobilized enzymes, PAM was a good flocculation agent, by which the size and its distribution was monomodal. The uniform and flexible environment of microstructured mesoporous materials led to a homogeneous distribution of the enzymes.

3.4. Kinetic Studies of Enzymatic Reaction for GDH and PDOR in Microfloccules. Characteristics of catalytic kinetic possibly caused by the immobilization were further investigated. The apparent Michaelis constants K_m and the maximum reaction rates V_{max} values of free and immobilized enzyme were measured by using either NAD^+ or glycerol as substrates, respectively. Figure 10 shows the Lineweaver–Burk plot for the NAD^+ reduction (A, 0.05–0.25 mM) and glycerol oxidation (B, 2.5–10 mM) with free and immobilized GDH. The V_{max} and K_m determined from Figure 10 are presented in Table 2. It is obvious that, for the substrate of both NAD^+ and glycerol, K_m of the immobilized GDH was slightly higher than that of the free GDH.

As we know, K_m related to the affinity of substrate molecule and enzyme. The smaller K_m the more affinity is. V_{max} reflects the scale of mass-transportation.[45] Therefore, the above result implies that the substrate concentration needed for the immobilized GDH was higher than that for the free counterpart. Moreover, the microfloccules affected the transport of substrate to GDH and the discharge of product. However, comparatively, the affinity was evidently affected. A little increase of V_{max} for the immobilized GDH was probably ascribed to the porous structure and hydrophilic surroundings of microfloccules. It was easier for substrate to diffuse through the pore channel and access to the enzymes. In contrast, the densely adsorbed enzymes hindered the contact of substrate with enzyme, namely decreased the affinity.

On the other hand, for the catalytic kinetics study for free and immobilized PDOR (eq 6), with the 1,3-PD concentrations from 10 to 50 mM (Figure 11A) and NAD^+ from 0.15 to 0.28 mM (Figure 11B), was shown in Table 3.

Both for free PDOR and immobilized PDOR, V_{max} and K_m were similar, namely that the apparently affinity of substrate 1,3-PD and PDOR faintly increased, whereas V_{max} nearly unchanged. These deviations were negligible in term of significance. Therefore, it indicated that the immobilization of PDOR in the microfloccules did not affect the properties of PDOR and the substrate diffusivity.

However, as for substrate of NAD^+, that V_{max} of free PDOR was larger than that of the immobilized, the lower V_{max} of immobilized PDOR may be ascribed to the steric hindrance of the active site by the support, and the loss of enzyme flexibility necessary for substrate binding or diffusion resistance to solute transport near the support.[46]

Nevertheless, the kinetic parameters indicated that the microfloccules with immobilized multienzyme catalyzed enzymatic reactions of 1,3-PD successfully. Under the reaction conditions of pH 8.0 and 37 °C, the highest yield of 1, 3-PD, 11.62 g/L in 10 h, was obtained by applying the microfloccules. It is practically applicable as an alternative of free enzyme in the industrial-scale production of 1,3-PD.

4. CONCLUSIONS

A facile and effective method to prepare relatively monodispersed microfloccules of TiO_2 nanoparticles with the immobilized multienzymes was demonstrated by using PAM as flocculation agent. Glycerol-dehydrogenase (GDH), 1,3-propanediol-oxidoreductase (PDOR) and glycerol-dehydratase (GDHt) were coimmobilized on hybrid PAM-TiO_2 carriers. PAM played a key role for forming microfloccules with relatively homogeneous distribution of size and reducing the enzyme leakage from the microfloccules during the catalysis reaction.

The temperature and pH as well as the amount of PAM and enzyme affected the loading and activity of immobilized enzymes. Loading amount as much as 104.1 mg/g of TiO_2 and >90% loading efficiency were obtained under the optimum conditions: 0.2 g of TiO_2, 20 mg of enzyme, 0.5 mg of PAM, pH 8.0, and 37 °C. Compared with the kinetic parameters of free enzymes, the immobilized enzymes exhibited similar biocatalytic behavior evidenced from their similar K_m and V_{max}.

The SEM/EDS observations suggested that the micro/nanoscale of immobilized multienzyme system is an important factor in determining their activities on dissimilation glycerol to 1,3-PD, and thus cofactor regeneration was proven feasible in this NAD(H)-dependent redox system with the yield of 11.62 g/L for 1,3-PD.

These results indicated that the porous and easy-separation microfloccules of TiO_2 nanoparticles with immobilized multienzymes were efficient in term of catalytic activity as much as the free enzymes.

AUTHOR INFORMATION

Corresponding Author

*Tel: +86-25-52090619. Fax: +86-25-52090621. E-mail: wuminnj@163.com.

ACKNOWLEDGMENT

This project is supported by National Natural Science Foundation of China (NSFC), Grant 51073035.

REFERENCES

(1) Zeng, A. P.; Biebl, H. *Adv. Biochem. Eng. Biotechnol.* **2002**, *74*, 239–259.
(2) Papanikolaou, S.; Fakas, S.; Fick, M.; Chevalot, I.; Galiotou-Panayotou, M.; Komaitis, M.; Marc, I.; Aggelis, G. *Biomass Bioenergy* **2008**, *32*, 60–71.
(3) Nakamura, C. E.; Whited, G. M. *Curr. Opin. Biotechnol.* **2003**, *14*, 454–459.
(4) Németh, Á.; Sevella, B. *Appl. Biochem. Biotechnol.* **2008**, *144*, 47–58.
(5) Wang, W.; Sun, J. B.; Hartlep, M.; Deckwer, W. D.; Zeng, A. P. *Biotechnol. Bioeng.* **2003**, *83*, 525–536.
(6) Mu, Y.; Teng, H.; Zhang, D. J.; Wang, Z. L. *Biotechnol. Lett.* **2006**, *28*, 1755–1759.
(7) El-Zahab, B.; Donnelly, D.; Wang, P. *Biotechnol. Bioeng.* **2008**, *99*, 508–514.
(8) Wichmann, R.; Vasic-Racki, D. *Adv. Biochem. Eng. Biotechnol.* **2005**, *92*, 225–260.
(9) Wang, P.; Ma, G. H.; Gao, F.; Liao, L. *China Part.* **2008**, *3*, 304–309.
(10) El-Zahab, B.; Jia, H. F.; Wang, P. *Biotechnol. Bioeng.* **2004**, *87*, 178–183.
(11) Ikemoto, H.; Chi, Q.; Ulstrup, J. *J. Phys. Chem. C* **2010**, *114*, 16174–16180.
(12) Kim, J. B.; Grate, J. W.; Wang, P. *Trends Biotechnol.* **2008**, *26*, 639–646.
(13) Yan, M.; Ge, J.; Liu, Z.; Ouyang, P. K. *J. Am. Chem. Soc.* **2006**, *124*, 11008–11009.
(14) Morimoto, N.; Endo, T.; Ohtomi, M.; Iwasaki, Y.; Akiyoshi, K. *Macromol. Biosci.* **2005**, *8*, 710–716.
(15) Vertegel, A. A.; Siegel, R. W.; Dordick, J. S. *Langmuir* **2004**, *20*, 6800–6807.
(16) Wang, P. *Curr. Opin. Biotechnol.* **2006**, *17*, 574–579.
(17) Xu, S. W.; Lu, Y.; Jiang, Z. Y.; Wu, H. *J. Mol. Catal. B: Enzym.* **2006**, *43*, 68–73.
(18) Jia, H.; Zhu, G.; Wang, P. *Biotechnol. Bioeng.* **2003**, *84*, 406–414.
(19) Reisner, E.; Fontecilla-Camps, J. C.; Armstrong, F. A. *Chem. Commun. (Cambridge, U. K.)* **2009**, *5*, 550–552.
(20) Xu, Z.; Liu, X. W.; Ma, Y. S.; Gao, H. W. *Environ. Sci. Pollut. Res.* **2010**, *17*, 798–806.
(21) Ohnuki, H.; Honjo, R.; Endo, H.; Imakubo, T.; Izumi, M. *Thin Solid Films* **2009**, *518*, 596–599.
(22) Gianotti, E.; Bertolino, C. A.; Benzi, C.; Nicotra, G.; Caputo, G.; Castino, R.; Isidoro, C.; Coluccia, S. *ACS Appl. Mater. Interfaces* **2009**, *1*, 678–687.
(23) Liu, L.; Shang, L.; Guo, S.; Li, D.; Liu, C.; Qi, L.; Dong, S. *Biosens. Bioelectron.* **2009**, *25*, 523–526.
(24) Kim, J.; Grate, J. W. *Nano Lett.* **2003**, *3*, 1219–1222.
(25) Jiang, Y. J.; Gao, Q. M. *J. Am. Chem. Soc.* **2006**, *128*, 716–717.
(26) Yang, B. H.; Xu, H. Y.; Yang, Z. Z.; Zhang, C. *J. Mater. Chem.* **2010**, *20*, 2469–2473.
(27) Sun, Q. Y.; Jiang, Y. J.; Jiang, Z. Y.; Zhang, L.; Sun, X. H.; Li, J. *Ind. Eng. Chem. Res.* **2009**, *48*, 4210–4215.
(28) Vaidya, B. K.; Ingavle, G. C.; Ponrathnam, S.; Kulkarni, B. D.; Nene, S. N. *Bioresour. Technol.* **2008**, *99*, 3623–3629.
(29) Kim, J.; Lee, J.; Na, H. B.; Kim, B. C.; Youn, J. K.; Kwak, J. H.; Moon, K.; Lee, E.; Kim, J.; Park, J.; Dohnalkova, A.; Park, H. G.; Gu, M. B.; Chang, H. N.; Grate, J. W.; Hyeon, T. *small* **2005**, *1*, 1203–1207.
(30) Hong, J.; Xua, D.; Gong, P.; Ma, H.; Dong, L.; Yao, S. *J. Chromatogr., B: Anal. Technol. Biomed. Life Sci.* **2007**, *850*, 499–506.
(31) Ahrens, K.; Menzel, K.; Zeng, A. P.; Deckwer, W. D. *Biotechnol. Bioeng.* **1998**, *59*, 544–552.
(32) Wu, M.; Yang, T. J.; Miao, M. D.; Ni, J. B. *Acta Chim. Sin.* **2009**, *67*, 2133–2138.
(33) Chen, H. W.; Wang, W.; Fang, B. S.; Wu, Z. D. *J. Chem. Eng. Chin. Univ.* **2004**, *18*, 621–627.
(34) Moniruzzaman, M.; Kamiya, N.; Goto, M. *Org. Biomol. Chem.* **2010**, *8*, 2887–2899.
(35) Yang, G.; Wu, J.; Xu, G.; Yang, L. *Bioresour. Technol.* **2009**, *100*, 4311–4316.
(36) Runkana, V.; Somasundaran, P.; Kapur, P. C. *J. Colloid Interface Sci.* **2004**, *270*, 347–358.
(37) Ni, H. M.; Kawaguchi, H. *J. Polym. Sci., Part A: Polym. Chem.* **2004**, *42*, 2823–2832.
(38) Ni, H. M.; Wu, M.; Li, M.; Wang, H.-L.; Sun, Y.-M. *Polym. Chem.* **2010**, *1*, 899–907.
(39) Nasser, M. S.; James, A. E. *Sep. Purif. Technol.* **2006**, *52*, 241–252.
(40) Solberg, D.; Wagberg, L. *Colloids Surf., A* **2003**, *219*, 161–172.
(41) Taylor, M. L.; Morris, G. E.; Self, P. G.; Smart, R. S. C. *J. Colloid Interface Sci.* **2002**, *250*, 28–36.
(42) Vertegel, A. A.; Richard, W. *Langmuir* **2004**, *20*, 6800–6807.
(43) Liu, P.; Xing, G. W.; Li, X. W.; Ye, Y. H. *Acta Phys.-Chim. Sin.* **2010**, *26*, 1113–1118.
(44) Yu, J. G.; Zhao, L.; Cheng, B. *Mater. Chem. Phys.* **2006**, *96*, 311–316.
(45) Wilson, D. J.; Aldrich, C. C. *Anal. Biochem.* **2010**, *404*, 56–63.
(46) Yan, J.; Pan, G.; Ding, C.; Quan, G. *Colloids Surf., B* **2010**, *79*, 298–303.